Microdynamics of Reverse Micelles of ω- and α,ω-Metal Sulfonato Polystyrene in Toluene

P. Vanhoorne,[†,‡] J. Grandjean,[§] and R. Jérôme*,[†]

Center for Education and Research on Macromolecules, University of Liège, Sart-Tilman B6, B-4000 Liège, Belgium

Received October 21, 1994; Revised Manuscript Received February 24, 1995[⊗]

ABSTRACT: Reverse micelles of ω- and α,ω-metal sulfonato polystyrenes in toluene have been investigated by ^{6}Li, ^{7}Li, and pulsed field gradient NMR. Micelles are found to be of a narrow size distribution and to consist of roughly spherical ionic cores shielded from the solvent by a polystyrene shell. The nature of the ion pair is found to influence significantly the micellar size. The correlation time characteristic of lithium relaxation is faster than the reorientational correlation time of the aggregates, which means that lithium relaxation essentially takes place within the ionic cores. The effective relaxation mechanism is consistent with a fast exchange of lithium ions between different coordination sites within the aggregates. In concentrated solutions, the equilibrium between aggregated polymer chains and unassociated chains is essentially shifted toward the aggregated species. This tendency is reversed upon dilution. Below a critical micellar concentration of ca. 0.01 g/dL, only "free" chains persist in solution. Temperature has no significant effect on the position of the aggregation equilibrium. The aggregates are dissociated by the addition of a polar cosolvent, such as methanol, which solvates the ion pairs. The MeOH/Li^+ molar ratio must, however, be higher than 100 to perturb significantly the ion pair aggregation. Up to a MeOH/Li^+ ratio of 10 000, part of the chains remain aggregated, and the lithium spin–lattice relaxation is dominated by the aggregates. Above a MeOH/Li^+ ratio of 10 000, the aggregates are almost completely disrupted. Self-diffusion coefficients of the difunctional chains are not dramatically smaller compared to the monofunctional counterparts, even when solutions of difunctional compounds form a gel. This behavior might be explained by the percolation model applied to the aggregation process, with the pulsed field NMR experiment probing only the self-diffusion of the clusters in the sol phase of the gel.

Introduction

Over the last 30 years, the unique mechanical, rheological, and transport properties of ionomers have been exploited in a wide range of applications including thermoplastic elastomers, permselective membranes, oil-drilling fluids, antistatics, and recording and imaging systems.[1–4] The intrinsic properties of ionomers result from the intermolecular interactions of the constitutive ionic groups. Although a considerable body of experimental and theoretical work has focused on the structure of ionomers, details of their phase morphology are still debated. Most ionomers, indeed, result from a random copolymerization process or a postpolymerization functionalization reaction. As a result, the ionic groups are randomly distributed along the chains, which results in a broad distribution for the chain length between two near-neighbor ionic aggregates. Moreover, entanglements of the constitutive chains contribute to nonionic cross-links. The intrinsic molecular and supramolecular heterogeneity of random ionomers explains why the detailed analysis of their morphology is quite a problem.

A better understanding of ionomer morphology has resulted from the study of halato-telechelic polymers (HTP's), which are linear chains or star-shaped polymers selectively end-capped with an ionic group.[5–13] Well-controlled molecular parameters and architecture make HTP's very useful models for the more complex ionomers. HTP's are expected to form much more regular polymer networks which can be modified at will. Studies of these model compounds have provided a better insight of the key parameters that control the phase morphology.[6,13] Recent papers[14,15] have reported on strong experimental supports for the model recently proposed in 1990 by Eisenberg *et al.*[16] for the structure and properties of ionomers.

Due to a low ionic content, HTP's are readily soluble in organic solvents of low and medium polarity.[8] In apolar solvents, the ion-pair aggregation is, however, currently responsible for gelation of HTP solutions at concentrations greater than 1 or 2 g/dL. In order to avoid this source of complexity, the best model for the analysis of the ion-pair aggregation consists of linear chains bearing only one ionic end group per chain, i.e., halato-semitelechelic polymers (HSTP's). Indeed, these chains aggregate into reverse micelles, and the ion-pair aggregation is no longer perturbed by the elastic response of the chain segments connecting the ion pairs.

A combined analysis by SAXS[17,18] and light scattering[19] has shown that multiplets formed by ω-metal sulfonato polystyrene keep their size and shape unchanged from the bulk state down to a 0.1 g/dL concentration in toluene and cannot be distinguished from multiplets formed by the α,ω-metal sulfonato counterparts. Static light scattering data[19] support an aggregation process that fits a closed association model, and the critical micellar concentration has been estimated to ca. 0.1 g/L. The average aggregation number slowly decreases as the molecular weight increases, which is in favor of a highly ordered structure for the ionic cores. The most stable structure has been found to consist of 12 lithium sulfonate ion pairs. As molecular weight increases, polymer–solvent interactions progressively distort the preferred ionic core structure, and above a critical molecular weight, estimated at 50 000 in toluene, multiplets collapse and smaller aggregates of ca. three ion pairs are formed.

Although the morphology of sulfonato-telechelic polymers is quite well understood, little is known about their

† Center for Education and Research on Macromolecules (CERM).
‡ Research assistant by the Belgian "National Fund for Scientific Research" (FNRS).
§ Laboratoire de Chimie Fine aux Interfaces.
⊗ Abstract published in *Advance ACS Abstracts,* April 1, 1995.

0024-9297/95/2228-3553$09.00/0

dynamics, both in bulk and in solution. This characteristic feature is, however, of the utmost importance when viscoelastic properties are concerned. For instance, melt viscosity and shear thickening of solutions in an apolar solvent are related to the dynamics of the ion-pair exchange. Moreover, contradictory results have been published on ionomers, that might be due to the nonequilibrium state of the samples. Reproducible results can only be obtained when the equilibration time is long enough compared to the time scale for the molecular rearrangements, which must therefore be investigated.

Recently, dynamics of the ion-pair interchange in solutions of randomly sulfonated polystyrene have been investigated by fluorescence techniques.[20,21] However, due to the ill-defined molecular parameters of random ionomers, it is not clear whether these results can be extended to any sulfonated polystyrene ionomer. Moreover, fluorescence measurements require big organic fluorescent probes to be incorporated into the ionic aggregates, which might considerably disturb both the structure and dynamics of the investigated system. In contrast to fluorescence measurements, NMR is a noninvasive technique that can provide both structural and dynamic information on a wide range of materials. Alkaline-metal NMR has particularly been used for probing the ion dynamics in various systems.[22−28] In this paper, the ion dynamics of solutions of ω- and α,ω-metal sulfonato polystyrenes in toluene will be investigated by means of lithium NMR. The well-defined molecular and supramolecular structure of these materials is expected to allow the effect of the main molecular parameters to be ascertained. The identified dynamic processes will be related to the supramolecular structure and the self-diffusion coefficients measured by pulsed field gradient NMR.

Experimental Section

Sample Preparation. ω-Metal and α,ω-metal sulfonato polystyrene samples were synthesized by living anionic polymerization of styrene followed by deactivation with 1,3-propanesultone, as reported elsewhere.[17] Functionality was systematically better than 90%, as checked by potentiometric titration of the acid end groups with a standard solution of tetramethylammonium hydroxide in a toluene/methanol (9/1, v/v) mixture.

Molecular weight and molecular weight distribution were measured by size-exclusion chromatography of a polymer sample picked out before deactivation of the living chains by 1,3-propanesultone.

Lithium sulfonate terminated polymers were purified by a repeated precipitation in methanol. For ^{6}Li NMR, lithium-7 sulfonate terminated polymers were converted into the sulfonic acid counterparts by a repeated precipitation in methanol containing at least 20 equiv of perchloric acid and a final reprecipitation in pure methanol. (Semi)telechelics were kept in the acid form in a toluene/methanol solution. The sulfonic acid end groups were neutralized by 1.05 equiv of lithium-6 acetate. Methanol and acetic acid were removed by the azeotropic distillation of the solvent (regularly replaced by dry toluene), until no polar compound could be detected in the distillate by gas chromatography and/or potentiometric titration. The solvent was finally removed by distillation. Both ^{7}Li and ^{6}Li samples were dried at 160 °C, under vacuum, for 16 h.

Unless otherwise stated, solutions were prepared by dissolving a weighed amount of polymer in a precise amount of toluene (analytical grade) in tight flasks with stirring for at least 1 day at 25 °C.

The samples were labeled as follows: the chain functionality (either 1 or 2), followed by the cation symbol, the number-average molecular weight in thousands, and the weight concentration of the polymer in toluene.

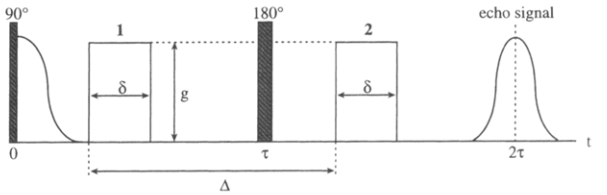

Figure 1. Pulse sequence used in the measurement of self-diffusion coefficients.

NMR Measurements. Lithium NMR. Both ^{6}Li and ^{7}Li NMR experiments were conducted on a Bruker AM-300 WB spectrometer operating at 44.168 and 116.643 MHz, respectively. The signal of 1 M aqueous LiCl was taken as an extenal reference in both cases. Unless otherwise stated, the temperature was fixed at 329 K. The effect of the magnetic field strength on the longitudinal relaxation time was checked by repeating some measurements on a Bruker AM-400 spectrometer operating at 155.524 MHz for ^{7}Li.

All solutions were prepared with analytical-grade toluene, and experiments with deuterated toluene showed that relaxation times were unaffected by the dipolar relaxation due to the surrounding protons.

The longitudinal relaxation time T_1 was measured by means of a simple inversion−recovery sequence using variable delay times (13 data points).

The apparent spin−spin relaxation time T_2^* was calculated from the width at half-height of the NMR lines according to eq 1. Since this value could be affected by the sample

$$T_2^* = 1/\pi\Delta\nu_{1/2} \tag{1}$$

microheterogeneity, T_2^* has also been measured with the Carr−Purcell−Meiboom−Gill pulse sequence (9 data points).

The two-dimensional double quantum spectrum was recorded with the pulse sequence $90_x-\tau/2-180_y-\tau/2-90_x-t_1-90_x-t_2$, as described elsewhere.[29]

Pulsed field gradient NMR. Self-diffusion coefficients were measured with the pulsed field gradient technique,[30−32] using a commercial pulsed field gradient probe and generator (Bruker) operating at a ^{1}H resonance frequency of 300 MHz. The pulse sequence of Figure 1 was used with pulsed field strengths, g, ranging from 0.19 to 2.1 T/m. Pulsed field duration δ was set to 7 ms, and time interval Δ was 35 ms ($D < 2 \times 10^{-11}$ m^2 s^{-1}) or 28 ms ($D > 2 \times 10^{-11}$ m^2 s^{-1}). Pulsed field strengths were calibrated on D_2O at 25 °C, assuming $D = 1.9 \times 10^{-9}$ m^2 s^{-1} for HDO in D_2O.[33] The self-diffusion coefficient of n-octanol was measured to check the accuracy of the measurements in the range of $D = 10^{-10}-10^{-11}$ m^2 s^{-1}. The experimental data agreed within 5% with the value reported by Herden *et al.*[34] ($D = 1.9 \times 10^{-10}$ m^2 s^{-1} at 20 °C).

All the solutions investigated by pulsed field gradient NMR were prepared as detailed above, except that toluene-d_8 (99.5% D, Janssen) was used in order to reduce the contribution of the solvent to the overall NMR signal. Nevertheless, solutions investigated in this study showed a biexponential decrease in intensity with increasing pulsed field strength, and the data were accordingly fitted to eq 2 where γ is the magnetogyric

$$I = I_1 \exp(-\gamma^2\delta^2g^2D_1(\Delta - {}^1/_3\delta)) + I_2 \exp(-\gamma^2\delta^2g^2D_2(\Delta - {}^1/_3\delta)) \tag{2}$$

ratio of the ^{1}H nucleus, δ is the pulsed field duration, g is the pulsed field strength, Δ is the time interval between the two gradient pulses (see Figure 1), and D_n and I_n are self-diffusion coefficients and line intensities, respectively. Nineteen experimental points were used to fit eq 2.

The fast self-diffusion coefficient was identified to that of toluene and attributed to residual (partly) hydrogenated toluene in toluene-d_8. Therefore, only the low diffusion coefficients, characteristic of polystyrene self-diffusion, are reported and discussed in this paper. All values are the average of at least three independent measurements.

Theory

Nuclei with a spin quantum number $I > {}^1/_2$ ($I = 1$ and ${}^3/_2$ for ^{6}Li and ^{7}Li, respectively) have a quadrupole

moment (eQ) which interacts with the electric field gradient at the nucleus (eq) produced by the electronic environment. Fluctuations of this quadrupolar interaction due to molecular motion are responsible for relaxation of these nuclei.

The ^{6}Li nucleus with a spin quantum number of 1 is characterized by longitudinal (R_1) and transverse (R_2) relaxation rates as given by[35]

$$R_1 = 6K[J(\omega_0) + 4J(2\omega_0)] \quad (3)$$

$$R_2 = 3K[3J(0) + 5J(\omega_0) + 2J(2\omega_0)] \quad (4)$$

where

$$J(n\omega_0) = \frac{\tau_c}{1 + (n\omega_0\tau_c)^2} \quad (5)$$

is the spectral density. K depends on the quadrupole coupling constant χ and the asymmetry parameter of the electric field gradient, η:

$$K = \frac{\pi^2\chi^2}{20}\left(1 + \frac{\eta^2}{3}\right) \quad (6)$$

with

$$\chi = \frac{e^2qQ}{h} \quad \text{and} \quad \eta = \frac{V_{xx} - V_{yy}}{V_{zz}} \quad (7)$$

The corresponding relaxation behavior is monoexponential, and the resulting line shape is Lorentzian, as has been established by Abragam.[35] With a spin quantum number of $^3/_2$, the ^{7}Li nucleus, by contrast, shows a biexponential relaxation in the nonextreme narrowing limit, i.e., when the product of the correlation time τ_c for the relaxation process and the Larmor frequency (ω_0) is larger than 1 ($\omega_0\tau_c > 1$). Longitudinal (R_1) and transverse (R_2) relaxation rates can then be expressed as the sum of a slow (s) and a fast (f) component:[36]

$$R_1 = 4K[0.2J(\omega_0) + 0.8J(2\omega_0)] = {}^1/_5R_{1,f} + {}^4/_5R_{1,s} \quad (8)$$

$$R_2 = 2K[0.6J(0) + J(\omega_0) + 0.4J(2\omega_0)] = {}^3/_5R_{2,f} + {}^2/_5R_{2,s} \quad (9)$$

The resulting non-Lorentzian line shape can be deconvoluted into two components, and the ratio of $R_{2,f}$ and $R_{2,s}$ allows τ_c to be estimated.

More elaborate models, mostly based on the so-called "two-site" model, have been reported in the literature.[28] Due to the small microheterogeneity of the samples, however, these models are not suited for the analysis of the present systems. The limited number of available experimental parameters characterizing each system (T_1*, T_2*, $T_{2,s}$, $T_{2,f}$) prevented us from using even more sophisticated models. For this reason and since a more detailed analysis of the data is not likely to change the qualitative conclusions of the present study, all the data have been analyzed on the basis of eqs 8 and 9.

Since contribution of the fast component to the spin–lattice relaxation rate is rather weak, a pseudomonoexponential decay of the magnetization is measured when $R_{1,f}$ and $R_{1,s}$ are not too much different, with R_1* with $^4/_5R_{1,s} + {}^1/_5R_{1,f}$. Comparison of R_1* with $R_{2,s}$ or $R_{2,f}$ is an alternate method to calculate τ_c. From the knowledge of τ_c and R_1*, the quadrupole coupling constant χ can also be estimated, which yields information on the symmetry of the environment.

Whenever the difference between $R_{2,s}$ and $R_{2,f}$ is large, the fast component gives rise to a very broad line which may be difficult to distinguish from the experimental noise and may remain undetected.[37] However, the biexponential behavior is still present and allows multiquantum coherences to be detected.[29,37] Therefore, observation of double-quantum coherences is, for instance, a clear indication of the nonextreme narrowing condition ($\omega_0\tau_c > 1$) even when the NMR lines appear to be Lorentzian in shape.

Table 1. Molecular Characteristics of ω- and α,ω-Metal Sulfonato Polystyrenes

M_n	$\bar{M}_w$	fty[a]
1000	1100	0.92
3000	3500	0.95
7000	8000	0.95
8500	9000	0.98
13000	14000	0.96
18500	19500	0.92
7200	9000	1.95
23500	25000	1.86

[a] Average number of sulfonate end groups per chain.

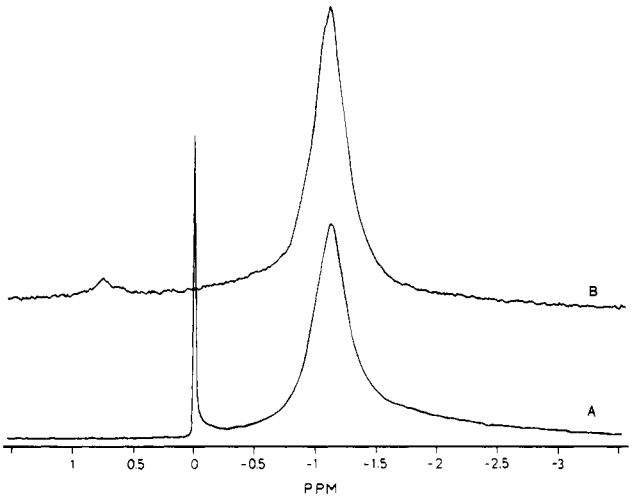

Figure 2. High-resolution ^{7}Li NMR spectra of (A) 1Li8K10 and (B) 1Li13K10 in toluene (concentration is 10 wt %, and T = 329 K). The reference is a 1 M aqueous solution of LiCl.

Results and Discussion

Solutions of a series of ω- and α,ω-lithium sulfonato telechelic polystyrenes in toluene have been analyzed by ^{7}Li and ^{6}Li NMR in the concentration range of 0.05–10 wt %. The molecular characteristics of these samples are listed in Table 1. Molecular weight distribution does not exceed 1.2, and functionality in the sulfonate is systematically better than 90% and 185% for mono- and difunctional samples, respectively.

Aggregate Structure. Typical ^{7}Li NMR spectra of 10 wt % solutions of ω-lithium sulfonato polystyrene in toluene are shown in Figure 2. Clearly, a fairly broad peak centered on −1.05 ppm dominates the whole spectrum. Previous light scattering measurements[19] have shown that this type of polymer forms reverse micelles in toluene at concentrations higher than 0.01 wt %. This signal has thus been assigned to the aggregated lithium cations. This assignment qualitatively agrees with solid-state ^{23}Na NMR analysis of random sulfonated ionomers,[38,39] which report negative chemical shifts for the aggregated Na ions.

In some cases, a weak signal centered at ca. 0.75 ppm is observed at low fields (Figure 2B), which is attributed

Table 2. Spectral Data for a Series of ω-^{6}Lithium Sulfonato Polystyrenes (10 wt % in Toluene)

$\bar{M}_n$	δ (ppm)	T_2* (ms)[a]
1000	−1.02	12.3
3000	−0.99	16.6
7000	−1.05	16.9
8500	−1.09	16.9
13000	−1.01	20.9
18500	−0.70	15.7
23500[b]	−1.03	25.7

[a] Calculated from the width at half-height. [b] Difunctional sample.

to smaller aggregates or nonaggregated ion pairs, as confirmed by dilution experiments (see below). That a single NMR signal is observed for the aggregated species is in favor of aggregates of a very similar structure, in accordance with the light scattering results, which also support a well-defined structure for the aggregates.[19] Moreover, assuming that NMR is able to discriminate the unassociated ion pairs from the aggregated ions (Figure 2B), the exchange between free and aggregated chains has to be slower than the NMR time scale, i.e., ca. 2 ms.

A better insight into the internal structure of the ionic aggregates should result from the replacement of $^7Li^+$ cations by $^6Li^+$ ones. Indeed, ^{6}Li NMR spectra are characterized by narrower lines compared to the parent ^{7}Li NMR spectra, due to the smaller quadrupole moment of the ^{6}Li nucleus. This better resolution of ^{6}Li NMR allows very close resonances to be discriminated, that are unresolved in ^{7}Li NMR spectra. Since ^{6}Li isotopic abundance is as low as 6% and ^{6}Li has a lower magnetogyric ratio than ^{7}Li, ^{6}Li-enriched samples have been prepared in order to avoid exceedingly long accumulation times. ^{6}Li NMR spectra are expectedly very similar to ^{7}Li ones and are essentially characterized by a single peak associated to the aggregated lithium cations. Spectral data are reported in Table 2 for a series of ω-lithium sulfonato polystyrenes and one difunctional sample at 10 wt % in toluene. Chemical shift and line width at half-height for the peaks characteristic of the monofunctional chains do not significantly depend on molecular weight in the investigated range, excepted for the chemical shift of the longest chains, which is moved downfield compared to the other samples. This gives credit to the previously reported light scattering results,[19] which concluded to the small dependence of the aggregate size on molecular weight in the same range. Table 2 also shows that the structure of the aggregates is the same for mono- and difunctional chains, which also agrees with SAXS data.[17,18] Conclusions drawn for the halato-semitelechelic polymers may thus be safely extended to halato-telechelic counterparts.

A ^{6}Li nucleus has a spin quantum number of 1, and no biexponential relaxation is expected to occur when $\omega_0\tau_c$ is larger than 1 (see Theory). The ^{6}Li NMR lines are non-Lorentzian, however. This characteristic feature might result from the overlap of several Lorentzian peaks very close of each other and associated with lithium ions in slightly different chemical environments. Peaks can be deconvoluted into (at least) two constitutive components, separated from each other by 0.1−0.2 ppm. Since the resonance of the aggregated species is relatively narrow and does not much depend on molecular weight, the aggregates are thought to be quite monodisperse. Therefore, the presence of very close resonances in the ^{6}Li NMR spectra has been attributed to a small sample microheterogeneity, which could originate from the presence of slightly different aggregates in solution, i.e., slightly different aggregation numbers.

Table 3. Spin−Lattice Relaxation Time for 1Li7K10 as a Function of Temperature

T (K)	T_1* (ms)	T (K)	T_1* (ms)
297	375	329	211
317	254	342	158

Although ^{6}Li NMR spectra provide a better resolution, large T_1 values make relaxation measurements quite time-consuming. Moreover, the quadrupole moment of this nucleus is small, and other interactions, such as dipolar interactions, may provide other relaxation mechanisms. For these reasons, ^{6}Li has not been used for probing ion dynamics.

Ion Dynamics. The spin−lattice relaxation time T_1 is 153 ms for $^7Li^+$ in 1Li13K10 at 329 K. This value is observed in toluene and toluene-d_8, which means that quadrupolar relaxation dominates the relaxation mechanism. The T_1 value is much larger than the apparent spin−spin relaxation time T_2*, which is as low as 8.2 ms. This large difference between longitudinal and transverse relaxation times agrees with a nonextreme narrowing condition. This conclusion is confirmed by the temperature dependence of T_1, as reported in Table 3. Actually, the spin−lattice relaxation time decreases as temperature is increased, which is the expected behavior when $\omega_0\tau_c > 1$. As explained in the theoretical section, nuclei with a $^3/_2$ spin quantum number exhibit biexponential relaxation outside the extreme narrowed limit. The experimental NMR line thus results from the overlapping of a narrow contribution (slow process, 40% of the total intensity) and a broad one (fast process, 60%). Deconvolution of the experimental peak may give access to the two constitutive components. However, in this case, the observed peak is nearly Lorentzian, and the biexponential behavior has been ascertained by a two-dimensional double-quantum (2Q) experiment which has been performed with the 1Li13K10 sample. Double-quantum coherences of $^3/_2$ spin systems can be detected outside the extreme narrowed conditions, and the shape of the two-dimensional spectrum provides a clear indication on the NMR spectral behavior.[29,37] The double-quantum spectrum is particularly well-suited to detect broad resonances that may remain undetected in the single-quantum (1Q) spectrum.[29] The 2D2Q spectrum of 1Li13K10 is shown in Figure 3. A single peak is observed in both the 1Q and 2Q spectra, which confirms the presence of a homogeneous biexponential relaxation.[29]

With 1Li8K10, the ^{7}Li line shape is clearly super-Lorentzian and deconvolution may give access to the fast ($T_{2,f}$) and slow ($T_{2,s}$) transverse relaxation times. From the $T_{2,f}/T_{2,s}$ ratio, the characteristic correlation time τ_c of ^{7}Li can be calculated. Comparison of T_1* to T_2* (measured by the Carr−Purcell−Meiboom−Gill pulse sequence, see the Experimental Section) is an alternate way for calculating τ_c. Calculated correlation times are reported in Table 4 for the 1Li13K10 and 1Li8K10 samples. When comparing τ_c values, it should be stressed that T_2 values for the "slow" and "fast" relaxation processes are calculated from the line width of the deconvoluted peaks and are thus not directly accessible from the experimental spectra. Moreover, the superimposition of at least two signals arising from slightly different aggregates might increase the experimental line width and thus alter T_2 values. Therefore, the τ_c value based upon direct comparison of T_1* and T_2* values is expected to be more reliable. Nevertheless, for both samples τ_c is larger than the value for "free"

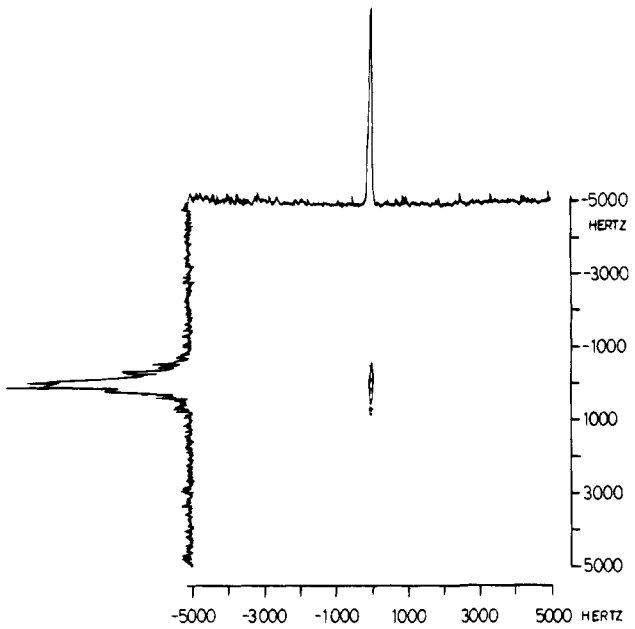

Figure 3. Two-dimensional double quantum ^{7}Li NMR spectrum of 1Li13K10 (T = 329 K). The top trace is the one-dimensional single-quantum spectrum, and the left trace is the one-dimensional double-quantum spectrum. A single peak in the two-dimensional plot is indicative of a biexponential relaxation.

Table 4. Experimental and Theoretical Correlation Times for 1Li13K10 and 1Li8K10

sample	τ_{c,T_1} (ns)[a]	τ_{c,T_2} (ns)[b]	$\bar{M}_w$	$R_{h,arm}$ (nm)[42]	$\bar{N}_w$[19]	$R_{h,star}$ (nm)	τ_r (ns)
1Li8K10	7.6	2.1	9000	2.1	11	3.5	25
1Li13K10	7.5		14000	2.7	9	4.5	51

[a] Calculated from the ratio T_1^*/T_2^*. [b] Calculated from the ratio $T_{2,f}/T_{2,s}$.

$^7Li^+$ cations in aqueous and polar organic solutions, which is on the order of 10^{-12}–10^{-11} s.[40] Clearly, the fluctuations of the electric field gradient, which are responsible for ^{7}Li quadrupolar relaxation, are much slower in the investigated systems than in aqueous solutions. It is worth pointing out that previous small-angle X-ray scattering and light scattering measurements[19] have shown that ω-lithium sulfonato polystyrene chains in toluene aggregate into reverse micelles that contain ca. 12 lithium sulfonate ion pairs, at least at concentrations higher than 0.01 wt %. Mobility of lithium cations embedded in the ionic core of reverse micelles should be drastically reduced compared to the motion of Li cations in polar solvents, as is experimentally observed.

Fluctuations of the electric field gradient surrounding the aggregated Li^+ cations might arise from the rotational reorientation of the whole aggregates. In this case, the correlation time for quadrupolar lithium relaxation would match the rotational correlation time of the aggregates. It has been shown that the aggregates are likely to be spherical, and the mean aggregation number has been measured for the samples under investigation.[19] The rotational correlation time for the spherical aggregates can be calculated by the Debye–Stokes–Einstein relationship:

$$\tau_r = 4\pi a^3 \eta / 3kT \qquad (10)$$

where a is the sphere radius and η the solvent viscosity. The radius a of the aggregates has been assumed to be the hydrodynamic radius, R_h. For an f arm star

Table 5. Dependence of Spectral Data for 1Li8K10 on the Addition of Methanol

C_{MeOH} (g/dL)	δ (ppm)	$T_{2,s}$ (ms)	$T_{2,f}$ (ms)	T_1^* (ms)
0	−1.09	10.2	2	153
0.01	−1.09	9.2	2.5	
0.1	−1.07	9.8	2.6	158
0.5		43.8	6	
1	−0.80	49.6	13.5	153
6	−0.50	289		1240

molecule, R_h can be calculated from eq 11.[41]

$$R_{h,star} = (3 - 2/f)^{1/2} R_{h,arm} \qquad (11)$$

From R_h values reported in the literature,[42] the rotational correlation times of the aggregates have been calculated and are reported in Table 4. Obviously, the correlation time for the lithium quadrupolar relaxation is significantly smaller than the rotational correlation time of the aggregates. Moreover, τ_c shows no dependence on the chain molecular weight, as would be expected for fluctuations associated with the aggregate rotation. Fluctuations of the electric field gradient are thus related to an internal rearrangement of the ionic core of the aggregates. This might be due to a fast association–dissociation process of the lithium sulfonate ion pairs or to a reorientation of the lithium environment within the aggregates. Since the lithium sulfonate ion pairs are known to be very stable,[17,18] the dissociation process is not expected to be favored, and quadrupolar lithium relaxation is likely to be due to a fast exchange of the lithium ions between slightly different coordination sites within the ionic core.

Further information on the lithium environment can be extracted from the quadrupole coupling constant, χ. For 1Li8K10, a χ value of 183 ± 20 kHz has been calculated, which is very large for lithium[43] and would indicate that the cation environment is highly asymmetric. This asymmetry might result from an irregular shape of the aggregates or from intrinsically asymmetric neighboring ions.

Ionic aggregation in most ionomers is known to be adversely affected by the addition of small amounts of a polar cosolvent, due to the ion-pair solvation.[1,3,13] Little is known, however, on the actual influence of polar cosolvents on the structure and dynamics of the ionic aggregates. ^{7}Li NMR has been used in order to investigate how far structure and dynamics of ω-lithium sufonatopolystyrene ionic aggregates in toluene depend on the addition of methanol. Spectral data for 1Li8K10 are reported in Table 5. Up to a 0.1 wt % concentration, methanol does not significantly disturb the ionic aggregates, since the chemical shift of the aggregated species and the transverse and longitudinal relaxation times remain unaffected. Above 0.5 wt % methanol, i.e., 13 methanol molecules per lithium sulfonate ion pair, the chemical shift moves downfield and the line width becomes narrower. No additional peaks for the solvated ions are observed in the spectrum (Figure 4). If, as is generally accepted, methanol is responsible for the ion-pair solvation, a single NMR peak indicates a fast exchange (on the NMR time scale) between aggregated and solvated ion pairs. Progressive dissociation of the ionic aggregates has been reported by Lundberg,[44] who, however, observed a constant viscosity in a wide temperature range for sulfonated-EPDM rubber solutions in xylene/hexanol and mineral oil/hexanol mixed solvents. The author explained this observation by a temperature-dependent equilibrium between rapidly

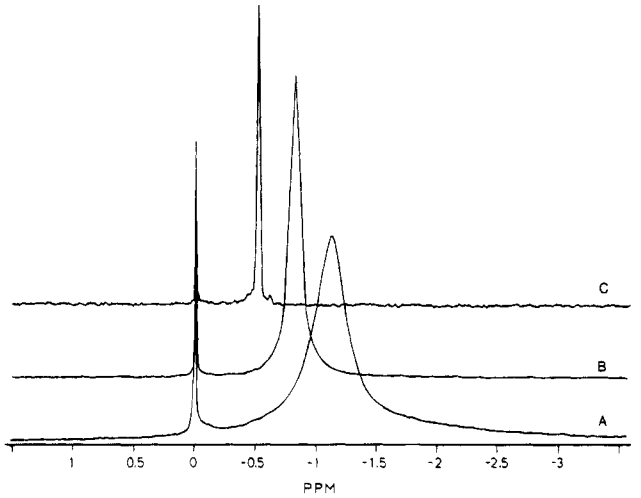

Figure 4. Effect of methanol on the ^{7}Li NMR signal for 1Li8K10 (T = 329 K). Methanol concentration (wt %) is (A) 0, (B) 1, and (C) 6 g/dL. The reference is a 1 M aqueous solution of LiCl.

exchanging aggregated and solvated metal sulfonate ion pairs, which is consistent with the results reported in this paper.

A decrease in the bandwidth is in agreement with a progressive increase in molecular dynamics. The NMR line becomes roughly Lorentzian at ca. 6 wt % methanol. In parallel, the spin–lattice relaxation time, T_1, becomes 1 order of magnitude larger, which reflects the effect of the lithium cation solvation. Together with an increased mobility, the solvated species are expected to be surrounded by quite a symmetric environment, leading to a relaxation time for the solvated ions longer than that for the aggregated species. Since the aggregated and solvated ions rapidly exchange at the NMR time scale, NMR essentially detects the faster process. The NMR time scale may be approximated from the difference in chemical shift for the aggregated and the solvated ion pairs. Cohen et al.[45] have reported a chemical shift of 0.5 ppm for lithium cations in a methanol solution, regardless of the counterion. Since the chemical shift for the aggregated species is −1.05 ppm, the difference in chemical shift is 1.55 ppm, i.e., 180 Hz at the 116.643 MHz Larmor frequency. Exchange processes are fast whenever the average lifetime of the nuclei in a single site, τ, obeys[46]

$$\tau < \sqrt{2}/\pi\Delta\nu \qquad (12)$$

i.e., τ < 2.5 ms. The average residence time of the lithium ions within the aggregates is thus in between a few nanoseconds (the lower limit being the quadrupole correlation time) and a few microseconds. At and above 6 wt % methanol, there is a decrease in the molar fraction of the aggregated species and/or in the average residence time of the ion pairs within the ionic core. Therefore, relaxation is dominated by the electric field fluctuations around the solvated ions. NMR results, however, are not in favor of a complete dissociation of the aggregates, even at a content of 6 wt % methanol. Indeed the longitudinal relaxation time goes on increasing with the amount of alcohol, as expected from a more extended dissociation of the aggregates.

Invariance of the aggregation behavior at low methanol concentration has also been confirmed by previous light scattering measurements,[19] as shown in Figure 5. The weight-average aggregation number of ω-lithium sulfonato polystyrene (M_n = 38 500) remains constant (and even increases slightly) up to a ratio of 100

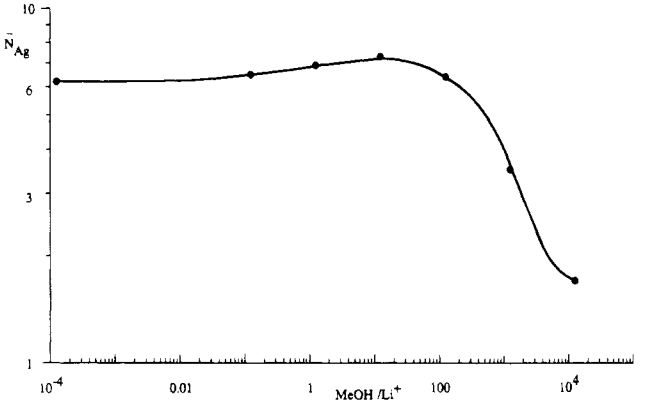

Figure 5. Effect of methanol on the average aggregation number, n, for ω-lithium sulfonato polystyrene (M_w = 39 500) in toluene at 300 K. Data were calculated from static light scattering measurements.[19] The solid line is a guide for the eyes.

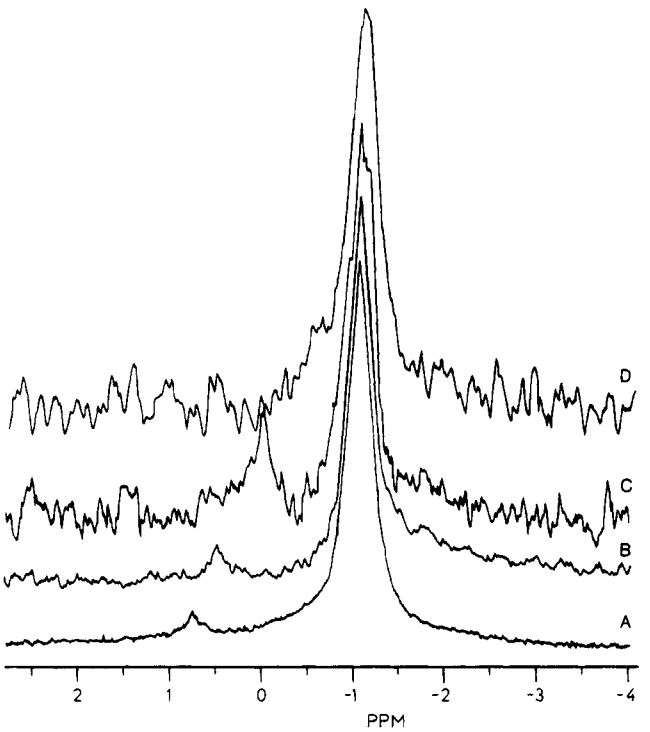

Figure 6. Variation of the NMR spectral lines with dilution for the 1Li13K sample in toluene at 329 K. Concentration (g/dL) is (A) 10, (B) 1, (C) 0.1, and (D) 0.05 g/dL.

methanol molecules/aggregate and then sharply decreases upon further addition of methanol. Even at a methanol content as high as 12 000 molecules/ion pair, aggregation is not completely disrupted (average aggregation number is 1.7). The agreement between both analytical methods is remarkably good. Up to 100 methanol molecules per ion pair, the reverse micelles remain essentially unaffected. Between 100 and 10 000 methanol molecules/ion pair, the average aggregation number of the micelles sharply decreases and the association–dissociation dynamics becomes faster. The ion pairs that are solvated by methanol remain isolated in solution. Above 10 000 methanol molecules/ion pair, the aggregates are almost completely disrupted in favor of single solvated ion pairs. The ionic aggregates are thus quite stable, since more than 100 methanol molecules/ion pair are required to destabilize dipole–dipole associations.

The concentration effect is shown in Figure 6 for the 1Li13K sample, and the related spectral data are listed in Table 6. Upon dilution, the relative intensity of the

Table 6. Dependence of Spectral Data for 1Li13K on Concentration and Temperature

conc (g/dL)	temp (K)	"aggregate" signal T_2^* (ms)[a]	"aggregate" signal intensity (%)[b]	"free" signal intensity (%)[b]	Δδ (ppm)
10	329	8.2	94 ± 2	6 ± 2	1.78
1	299	9.3	93 ± 2	7 ± 2	1.58
1	329	7.7	90 ± 2	10 ± 2	1.65
1	346	7.3	91 ± 2	9 ± 2	1.83
0.1	329	4.8	78 ± 2	22 ± 2	1.53
0.077	329	5.2			
0.05	329	7.5			

[a] Calculated from the width at half-height. [b] % of the total integrated intensity.

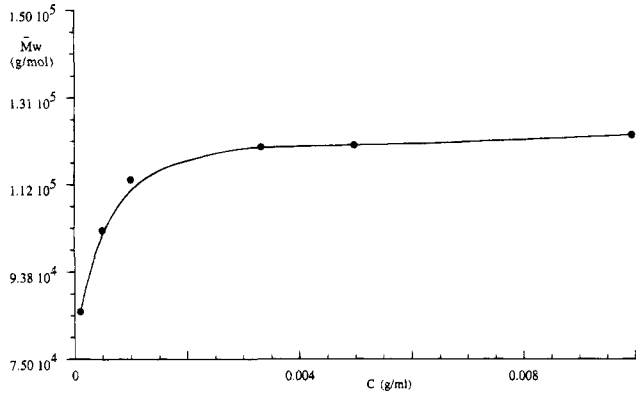

Figure 7. Weight-average molecular weight, $\bar{M}_w$, measured by static light scattering, as a function of concentration for 1Li13K, in toluene, at 300 K.[19]

peak corresponding to the aggregates progressively decreases in favor of the less aggregated species. Moreover, the two signals move to each other when dilution is increased, and they merge in a single signal below 0.1 wt %. This observation may be rationalized on the basis of faster exchanges between micelles and single chains upon dilution, so that the dynamic process is no longer slow on the NMR time scale. The average residence time of the ion pairs within the micelles decreases below 2 ms, and the NMR lines of the aggregates and the single chains coalesce progressively. Figure 6 shows that the exchange process is too fast for ^{7}Li NMR to detect two separate signals at polymer concentrations smaller than 0.1 wt %. Since aggregates remain the major species in solution, the chemical shift of the averaged NMR signal remains close to that of the reverse micelles. In a concentration range below 0.1 wt %, NMR is thus unable to give information on the relative proportion of aggregates and single chains, so that cmc can only be assumed to be lower than 0.1 wt %. This picture is in complete agreement with previous static light scattering measurements,[19] as shown in Figure 7. The weight-average molecular weight of the aggregates remains constant down to 0.1 g/dL in toluene, and then it sharply drops until reaching the molecular weight of single chains below 0.05 g/dL. Since static light scattering is sensitive to the *weight* fraction of the solute, a small fraction of unaggregated chains may remain undetected. In contrast, NMR is sensitive to the average *number* of particles and is therefore better suited to detect free chains.

Table 6 also exemplifies the temperature dependence of the aggregation equilibrium. Obviously, no significant change in the relative intensity of the peaks can be detected when the temperature is raised from 299 to 346 K. This observation is in agreement with the picture of stable aggregates and of an aggregation energy value much larger than kT. The difference in

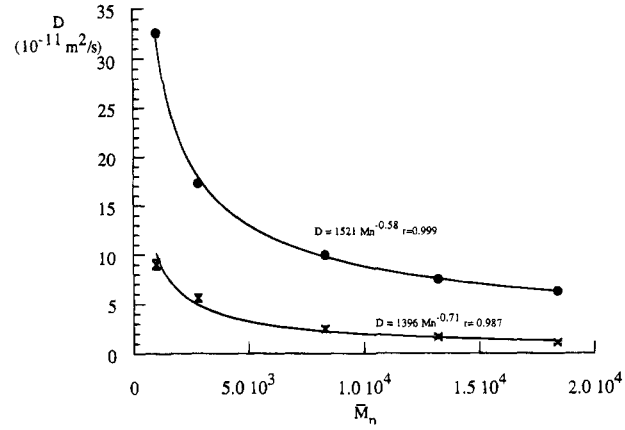

Figure 8. Dependence of the self-diffusion coefficient, D, on molecular weight for a series of ω-lithium sulfonato polystyrenes in toluene (×) and their parent unfunctionalized counterparts (●) (10 wt %, 298 K).

chemical shift between the two NMR peaks, however, increases at higher temperatures. A more detailed analysis shows that the chemical shift of the signal of the aggregated species remains unaffected, as is expected for stable aggregates. As a result, the signal of the unaggregated ion pairs is shifted downfield upon increasing temperature. This shift might arise from a change in the solvent quality which is detected by the single ion pairs, in contrast to the aggregated ion pairs which are shielded from the solvent by the polymer shell.

Self-Diffusion Measurements. Since the average residence time of the ion pairs in the aggregates is on the order of a few microseconds and since NMR hardly detects the unaggregated species, the polymer chains are detected as essentially small star-shaped aggregates. Therefore, self-diffusion of these aggregates should be measured, and the self-diffusion coefficient of ω-metal sulfonato polystyrenes in toluene should be significantly smaller than the self-diffusion coefficients of the parent unfunctionalized chains. Moreover, since parameters such as molecular weight and the nature of the ion pairs are known to influence the size of the reverse micelles, self-diffusion coefficients are also predicted to depend on the same parameters.

The self-diffusion coefficients for a series of ω-lithium sulfonated polystyrenes are plotted in Figure 8 and compared to the self-diffusion coefficients of unfunctionalized chains.[47] In all cases, the self-diffusion coefficients of the end-functionalized chains are much smaller than those of the correpsonding unfunctionalized counterparts, which is in complete agreement with the previously reported aggregation behavior of the functional chains.[19] Moreover, Figure 8 clearly shows that the self-diffusion coefficients of ω-lithium sulfonato polystyrenes in toluene scale with the molecular weight of the chains according to a power law (eq 13). The

$$D = K\bar{M}_n^{-0.71} \tag{13}$$

scaling exponent −0.71 observed for the starlike aggregates of ω-lithium sulfonato polystyrenes is significantly different from the scaling exponent of −0.58 reported by Huber et al.[42] for the self-diffusion of unfunctionalized polystyrene. This discrepancy might rely upon a different conformation of the chains in the reverse aggregates formed by ω-lithium sulfonato polystyrenes compared to the random-coil conformation of the unfunctionalized chains.

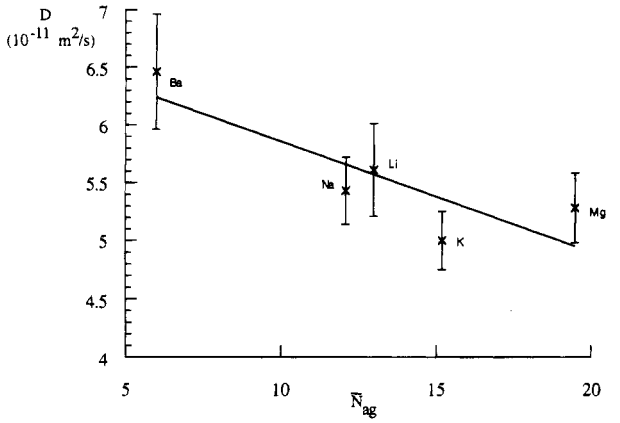

Figure 9. Dependence of the self-diffusion coefficient, D, on the aggregation number, $\bar{N}_{agg}$, for a series of ω-metal sulfonato polystyrenes ($\bar{M}_n$ = 3000, 10 wt % in toluene, 298 K). The line is a guide for the eyes.

Table 7. Effect of Methanol on the Self-Diffusion Coefficient of ω-Lithium Sulfonato Polystyrene ($\bar{M}_n$ = 8500, 10 wt % in Toluene, 298 K)

methanol (wt %)	D (10^{-11} m^2 s^{-1})	methanol (wt %)	D (10^{-11} m^2 s^{-1})
0	2.5 ± 0.3	6	3.5 ± 0.4
1	2.9 ± 0.2		

The effect of the ion pair on the self-diffusion coefficient of ω-metal sulfonato polystyrenes ($\bar{M}_n$ = 3000) is reported in Figure 9. The counterion of the sulfonate end groups influences the self-diffusion coefficient and thus the aggregation behavior of the investigated HSTP's. The fastest (and thus smallest) aggregates are formed when barium is the cation, whereas potassium and magnesium contribute to the slowest (and thus largest) aggregates. This behavior is consistent with the aggregation numbers previously measured by static light scattering.[19] Although aggregation numbers cannot be directly extracted from self-diffusion coefficients, the same trend is observed by pulsed field gradient NMR and static light scattering. In the ionic core of the reverse micelles, the ion pairs are accordingly thought to be arranged in a well-defined manner which strongly depends on the nature of both the cation and the anion. Therefore, no general model is expected to account for the aggregation behavior of all ionomers and halato-(semi)telechelic polymers. Rather, each ionomer (or at best each ionomer class) should be a case per se and should be investigated in detail in order to ascertain the exact size and shape of the ionic aggregates.

Since ^{7}Li NMR has shown that the ionic aggregates are partially disrupted by a polar solvent, such as methanol, the aggregate dissociation has been investigated by pulsed field gradient NMR. The effect of methanol on the self-diffusion coefficients of ω-lithium sulfonato polystyrene ($\bar{M}_n$ = 8500) is reported in Table 7. Increasing methanol concentration results is an increase of the self-diffusion coefficient of the polystyrene chains, which can be entirely explained by a progressive dissociation of the aggregates. Even at 6 wt % methanol (i.e., 150 MeOH molecules/lithium sulfonate ion pair), the aggregates are however, far from being completely disrupted, since the self-diffusion coefficient is still about 3 times smaller than that of the corresponding unfunctionalized (and thus unassociated) chains. Since similar behavior has been observed by ^{7}Li NMR and static light scattering results (see Table 5 and Figure 4), lithium sulfonate based aggregates appear to be quite stable against solvation with a polar solvent.

Table 8. Self-Diffusion Coefficients for Two α,ω-Metal Sulfonato Polystyrenes As Measured by Pulsed Field Gradient NMR in Toluene at 298 K

sample	D (10^{-11} m^2 s^{-1})	sample	D (10^{-11} m^2 s^{-1})
2Na7K10	1.9 ± 1	2Li23K10	0.5 ± 0.3
2Na7K1	4.9 ± 0.5		

Finally, the self-diffusion coefficients of α,ω-metal sulfonato polystyrenes has been examined in order to probe the influence of gelation on the local mobility of individual chains. Interestingly enough, self-diffusion of difunctional chains, although significantly slower, is not dramatically slowed down compared to that of monofunctional chains, as observed from Table 8 and Figure 8. This behavior may only be explained by a relatively fast chain exchange between aggregates during the self-diffusion coefficient measurement, i.e., ca. 30 ms (see the Experimental Section). Moreover, dissolution of the difunctional gel (dilution of the $\bar{M}_n$ = 7000 sample down to 1 wt % gives rise to a homogeneous solution) results in a moderate increase of the self-diffusion coefficient as a result of medium dilution. Therefore, in the polymer concentration range of a few weight percent, the local structure of the aggregates of difunctional chains is stable and the gelation process does not result from a pronounced modification in the local chain connectivity but rather from the interconnection of small clusters consisting of several ionic multiplets. This picture is in agreement with results collected by neutron and light scattering,[19,48] which highlight the complex aggregation of the difunctional chains and, particularly, the progressive association of individual multiplets into larger structures. Gelation would thus be adequately described by a percolation model,[49] based on the growth of aggregates until the whole solution is connected, which happens at the critical gel concentration. The percolation model, however, assumes that, even well above the critical gelation concentration, a significant fraction of aggregates is not connected to the gel fraction and forms an "internal" sol fraction. It is thus reasonable to accept that pulsed field gradient NMR only probes self-diffusion of the mobile fraction in the gel, which results in self-diffusion coefficients not dramatically smaller than those of the starlike aggregates formed by the monofunctional chains. This hypothesis is supported by absolute intensity measurements on 2Na23K in the gel state, which show that only 67% of the total ^{1}H intensity is detected by NMR when the polymer concentration reaches 3.3 wt %. The gel fraction, almost immobile, is characterized by such a small transverse relaxation time that NMR can no longer detect the corresponding signal (NMR invisibility). Upon dilution, the gel is destroyed, and the increase in the self-diffusion coefficient then merely reflects the dilution effect.

Conclusions

Lithium NMR and pulsed field gradient NMR of ω-lithium sulfonato polystyrene in toluene have confirmed the formation of reverse micelles and provided information on the structure and dynamics of the ionic cores. At high concentrations (i.e., above 0.1 wt %), metal sulfonate ion pairs are aggregated into small and roughly spherical cores. These ionic aggregates are essentially independent of the polystyrene molecular weight but are strongly dependent on the nature of the ion pair. ^{6}Li NMR showed that at least two different types of slightly different aggregates coexist, which might be attributed to a small difference in aggregation number. The quadrupolar relaxation of ^{7}Li has a

correlation time on the order of 7.5 ns, independent of molecular weight, which is shorter than the characteristic rotational correlation time for the reverse micelles (>25 ns). Lithium relaxation thus occurs within the ionic core of the micelles, and the basic relaxation mechanism would be diffusion of the lithium cations between different coordination sites within the same aggregate.

Exchange between reverse micelles and single chains is slow compared to the NMR time scale (2 ms), and the signal arising from the unassociated chains may be distinguished from the signal of the aggregated ion pairs. Upon dilution, the reverse micelles progressively dissociate into free chains. Below a critical micellar concentration which may be estimated to 0.1 wt %, reverse micelles are no longer stable and only single chains are present in solution.

The addition of methanol progressively solvates the lithium sulfonate ion pairs, which results in the disruption of the reverse micelles. These micelles are, however, quite stable, since methanol has no effect when less than 100 methanol molecules have been added per sulfonate ion pair. Between 100 and 10 000 methanol molecules/ion pair, a fast exchange between aggregated and solvated ion pairs occurs, although the spin–lattice relaxation is still dominated by the aggregates. Above a critical value of 10 000 methanol molecules/ion pair, the reverse micelles are completely disrupted in favor of the solvated ion pairs, and the spin–lattice relaxation time is 1 order of magnitude larger compared to the aggregates.

On the basis of ^{6}Li NMR measurements, the ionic aggregates in α,ω-lithium sulfonato polystyrenes cannot be distinguished from those formed in ω-lithium sulfonato polystyrenes. Pulsed field gradient NMR has, however, shown that the aggregation behavior of α,ω-lithium sulfonato polystyrenes is complex and involves an aggregation process which is best described by a percolation model.[49]

Acknowledgment. The authors are very much indebted to the "Services Fédéraux des Affaires Scientifiques, Techniques et Culturelles" (SSTC), Belgium, and to the Belgian National Fund for Scientific Research (FNRS, Brussels) for providing P.V. with a research assistantship and for the purchase of pulsed field gradient accessories.

References and Notes

(1) *Structure and Properties of Ionomers*; Pinéri, M., Eisenberg, A., Eds.; NATO Advanced Study Institute Series C198; Reidel: Boston, 1987.
(2) MacKnight, W. J.; Earnest, T. R. *J. Polym. Sci., Macromol. Rev.* **1981**, *16*, 41.
(3) *Coulombic Interactions in Macromolecular Systems*; Eisenberg, A., Bailey, F. E., Eds.; ACS Symposium Series 302; American Chemical Society: Washington, DC, 1986.
(4) *Ions in Polymers*; Eisenberg, A., Ed.; Advances in Chemistry Series 187; American Chemical Society: Washington, DC, 1980.
(5) Broze, G.; Jérôme, R.; Teyssié, Ph.; Gallot, B. *J. Polym. Sci., Polym. Lett. Ed.* **1981**, *19*, 415.
(6) Williams, C. E.; Russell, T. P.; Jérôme, R.; Horrion, J. *Macromolecules* **1986**, *19*, 2877.
(7) Broze, G.; Jérôme, R.; Teyssié, Ph. *Macromolecules* **1981**, *14*, 224.
(8) Broze, G.; Jérôme, R.; Teyssié, Ph.; Marco, C. *Polym. Bull.* **1981**, *4*, 241.
(9) Broze, G.; Jérôme, R.; Teyssié, Ph. *Macromolecules* **1982**, *15*, 920.
(10) Vlaic, G.; Williams, C. E.; Jérôme, R.; Tant, M. R.; Wilkes, G. L. *Polymer* **1987**, 29, 173.
(11) Bagrodia, S.; Pisipati, R.; Wilkes, G. L.; Storey, R. F.; Kennedy, J. P. *J. Appl. Polym. Sci.* **1984**, *29*, 3065.
(12) Fitzgerald, J. J.; Weiss, R. A. *J. Macromol. Sci., Rev. Macromol. Chem. Phys.* **1988**, *C28* (1), 99.
(13) Jérôme, R. In *Telechelic Polymers: Synthesis and Applications*; Goethals, E. J., Ed.; CRC Press, Inc.: Boca Raton, FL, 1989; Chapter 11.
(14) Yano, S.; Tadano, K.; Jérôme, R. *Macromolecules* **1991**, *24*, 6439.
(15) Vanhoorne, P.; Jérôme, R.; Teyssié, Ph.; Lauprêtre, F. *Macromolecules* **1994**, *27*, 2548.
(16) Eisenberg, A.; Hird, B.; Moore, R. B. *Macromolecules* **1990**, *23*, 4098.
(17) Vanhoorne, P.; Van den Bossche, G.; Fontaine, F.; Sobry, R.; Jérôme, R.; Stamm, M. *Macromolecules* **1994**, *27*, 838.
(18) Vanhoorne, P.; Maus, C.; Van den Bossche, G.; Fontaine, F.; Sobry, R.; Jérôme, R.; Stamm, M. *J. Phys. IV* **1993**, *3* (C8), 63.
(19) Vanhoorne, P.; Jérôme, R., submitted to *Macromolecules*.
(20) Morawetz, H.; Wang, Y. *Macromolecules* **1988**, *21*, 107.
(21) Dowling, K. C.; Thomas, J. K. *Macromolecules* **1991**, *24*, 4131.
(22) Lindman, B.; Forsen, S. *NMR Basic Principles and Progress*; Springer Verlag: Berlin, 1976; Vol. 12, Chapter 5.
(23) Johansson, C.; Drakenberg, T. *Ann. Rep. NMR Spectrosc.* **1989**, *22*, 1.
(24) Grandjean, J. *Ann. Rep. NMR Spectrosc.* **1992**, *24*, 181.
(25) Grandjean, J.; Laszlo, P. Quadrupolar Probes in Solution In *Dynamics in Solutions and Fluid Mixtures by NMR*; Delpuech, J. J., Ed.; John Wiley and Sons: London, in press.
(26) Grandjean, J.; Laszlo, P. *J. Magn. Reson.* **1991**, *92*, 404.
(27) Park, J.-K.; Park, B.-K.; Ryoo, R. *Polym. Eng. Sci.* **1991**, *31*, 873.
(28) Kenéz, P. H.; Carlström, G.; Furó, I.; Halle, B. *J. Phys. Chem.* **1992**, *96*, 9524.
(29) Rooney, W. D.; Barbara, T. M.; Springer, C. S., Jr. *J. Am. Chem. Soc.* **1988**, *110*, 674.
(30) Stejskal, E. O.; Tanner, J. E. *J. Chem. Phys.* **1965**, *42*, 288.
(31) Von Meerwall, E. D. *Adv. Polym. Sci.* **1983**, *54*, 1.
(32) Stilbs, P. *NMR Spectrosc.* **1987**, *19*, 1.
(33) Callaghan, P. T.; Le Gros, M. A.; Pinder, D. N. *J. Chem. Phys.* **1983**, *79*, 6372.
(34) Herden, H.; Kärger, J.; Pfeifer, H.; Kube, C.; Schöllner, R. *J. Colloid Interface Sci.* **1992**, *152*, 281.
(35) *The Principles of Nuclear Magnetism*; Abragam, R., Ed.; Clarendon: Oxford, U.K., 1970; Chapter VIII.
(36) Hubbard, P. S. *J. Chem. Phys.* **1970**, *53*, 985.
(37) Jaccard, G.; Wimperis, S.; Bodenhausen, G. *J. Chem. Phys.* **1986**, *85*, 6282.
(38) Komoroski, R. A.; Mauritz, K. A. *J. Am. Chem. Soc.* **1978**, *100*, 7487.
(39) McO'Connell, E.; Root, T. W.; Cooper, S. L. *Macromolecules* **1994**, *27*, 5803.
(40) Hertz, H. G.; Tutsch, R.; Versmold, H. *Ber. Bunsen-Ges. Phys. Chem.* **1971**, *75*, 1177.
(41) Jalal, V.; Duplessix, R. *J. Phys. (Fr.)* **1988**, *49*, 1775.
(42) Huber, K.; Bantle, S.; Lutz, P.; Burchard, W. *Macromolecules* **1985**, *18*, 1461.
(43) van der Klink, J. J.; Borsa, F. *Phys. Rev. B* **1984**, *30*, 52.
(44) Lundberg, R. D. *J. Appl. Polym. Sci.* **1982**, *27*, 4623.
(45) Cohen, Y. H.; Handy, P. R.; Roach, E. T.; Popov, A. I. *J. Phys. Chem.* **1975**, *79*, 80.
(46) *Modern NMR Spectroscopy*; Sanders, J., Hunter, B., Eds.; Oxford University Press: Oxford, U.K., 1990; Chapter 7.
(47) Self-diffusion coefficients at infinite dilution (D_0) are reported in ref 41 for polystyrene in toluene. The data at 10 wt % concentration have been calculated using $D = D_0(1 + k_D C)$.[42] $k_D = -0.045$ dL/g has been measured on unfunctionalized polystyrene ($\bar{M}_n$ = 8500) and has been assumed to be independent of molecular weight. The different values of Figure 8 have then been calculated on the basis of k_D and the data reported in ref 42.
(48) Timbó, A. M.; Higgins, J. S.; Peiffer, D. G.; Maus, C.; Vanhoorne, P.; Jérôme, R. *J. Phys. IV* **1993**, *3* (C8), 71.
(49) *Introduction to Percolation Theory*; Stauffer, D., Ed.; Taylor and Francis Ltd.: London, 1985.

MA9461308